Helper-Dependent Adenovirus Transduces the Human and Rat Retina but Elicits an Inflammatory Reaction When Delivered Subretinally in Rats

Ian C. Han,[1,2] Erin R. Burnight,[1,2] Mallory J. Ulferts,[1,2] Kristan S. Worthington,[1–3] Stephen R. Russell,[1,2] Elliott H. Sohn,[1,2] Robert F. Mullins,[1,2] Edwin M. Stone,[1,2] Budd A. Tucker,[1,2] and Luke A. Wiley[1,2,*]

[1]The University of Iowa Institute for Vision Research and [2]Department of Ophthalmology and Visual Sciences, Carver College of Medicine, University of Iowa, Iowa City, Iowa; [3]Department of Biomedical Engineering, University of Iowa, Iowa City, Iowa.

The identification of >100 genes causing inherited retinal degeneration and the promising results of recent gene augmentation trials have led to an increase in the number of studies investigating the preclinical efficacy of viral-mediated gene transfer. Despite success using adeno-associated viruses, many disease-causing genes, such as *ABCA4* or *USH2A*, are too large to fit into these vectors. One option for large gene delivery is the family of integration-deficient helper-dependent adenoviruses (HDAds), which efficiently transduce postmitotic neurons. However, HDAds have been shown in other organ systems to elicit an immune response, and the immunogenicity of HDAds in the retina has not been characterized. In this study, HDAd serotype 5 (HDAd5) was found to successfully transduce rod and cone photoreceptors in *ex vivo* human retinal organ cultures. The ocular inflammatory response to subretinal injection of the HDAd5 was evaluated using a rat model. Subretinal injection of HDAd5 carrying cytomegalovirus promoter-driven enhanced green fluorescent protein (HDAd5-CMVp-eGFP) elicited a robust inflammatory response by 3 days postinjection. This reaction included vitreous infiltration of ionized calcium-binding adapter molecule 1 (Iba1)-positive monocytes and increased expression of the proinflammatory protein, intercellular adhesion molecule 1 (ICAM-1). By 7 days postinjection, most Iba1-positive infiltrates migrated into the neural retina and ICAM-1 expression was significantly increased compared with buffer-injected control eyes. At 14 days postinjection, Iba1-positive cells persisted in the retinas of HDAd5-injected eyes, and there was thinning of the outer nuclear layer. Subretinal injection of an empty HDAd5 virus was used to confirm that the inflammatory response was in response to the HDAd5 vector and not due to eGFP-induced overexpression cytotoxicity. Subretinal injection of lower doses of HDAd5 dampened the inflammatory response, but also eGFP expression. Despite their larger carrying capacity, further work is needed to elucidate the inflammatory pathways involved and to identify an immunomodulation paradigm sufficient for safe and effective transfer of large genes to the retina using HDAd5.

Keywords: helper-dependent adenovirus, retina, inflammation

INTRODUCTION

Vision loss associated with inherited retinal degeneration commonly results from mutation-induced gene dysfunction that, in turn, causes death of photoreceptor cells. Since the human retina has limited regenerative capability, treatments designed to restore normal gene function and prevent photoreceptor cell loss are critical for the preservation of vision in those affected with inherited retinal disease. The recent clinical success of adeno-associated virus (AAV)-based gene augmentation for treatment of *RPE65*-associated Leber congenital amaurosis (LCA),[1–3] a form of severe early-onset photoreceptor cell degeneration, has paved the way for several other ocular gene-replacement trials (*e.g.*, *CHM*[4] and *RS1*[5]). A major constraint to this approach is that AAV vectors have a limited packaging capacity (~4.7 kb),[6]

*Correspondence: Dr. Luke A. Wiley, Department of Ophthalmology and Visual Sciences, Carver College of Medicine, University of Iowa, 375 Newton Road, Iowa City, IA 52242. E-mail: luke-wiley@uiowa.edu

DOI: 10.1089/hum.2019.159

which is far exceeded by several of the most common disease-causing genes. For instance, in a recent study of 1,000 consecutive families seen in an inherited retinal disease clinic at our institution, mutations in *ABCA4* and *USH2A* were the two most common causes of disease, and both of these genes are too large to package into AAV.[7]

Of the other viral vectors that have been tested in preclinical retinal gene transfer studies, lentiviruses have attracted significant attention. Lentiviral vectors, which have a packaging capacity of 8–10 kb,[6] have been used to deliver genes such as *CEP290* (~7.4 kb), *ABCA4* (~6.8 kb), and *MYO7A* (~6.6 kb) to models of LCA, Stargardt disease, and Usher syndrome, respectively.[8–10] Lentiviral equine infectious anemia virus also demonstrated ability to deliver robust and sustained transgene expression of endostatin and angiostatin in patients with neovascular age-related macular degeneration.[11] Although results have been encouraging, lentiviruses have several significant limitations, not the least of which is that they too have carrying capacities that are exceeded by the coding sequence of genes such as *USH2A* (~15.6 kb). In addition, lentiviruses have been reported to exhibit poor photoreceptor cell tropism[12,13] and can integrate within the host genome, creating the potential for harmful genotoxicity.[14,15]

Another option for packaging and delivery of large cDNAs are the episomal (*i.e.*, nonintegrating) helper-dependent adenoviruses (HDAds).[16] In contrast to first-generation adenoviruses, HDAds are "gutless vectors" that lack viral coding regions, allowing for a much larger cloning capacity (up to ~36 kb) and reduced immunogenicity.[17] As HDAds have been shown to efficiently transduce and mediate long-term transgene expression within postmitotic retinal neurons,[18,19] they are excellent candidates for delivery of retinal genes that exceed the carrying capacity of AAVs.[16,20] That said, although the lack of viral coding region should theoretically reduce the risk of a host immune response, there is evidence that HDAd-based therapeutic vectors can still elicit an immune reaction after delivery to the lungs and liver in mice.[21,22] Although an immune response in a tissue with regenerative properties, such as the liver, may have minimal long-term consequences, a similar response in the neural retina, where the majority of cells are terminally differentiated neurons, could be quite harmful. As such, despite potential as a large gene transfer vector for ocular diseases, the immunogenicity of HDAd in the retina needs to be fully characterized before clinical application.

In this study, we evaluate the transduction of HDAd serotype 5 (HDAd5—the most common serotype used for gene augmentation[23]) in human retinal explants and the immune response after subretinal delivery in rats with intact immune systems. We demonstrate that HDAd5 effectively transduces the retina but provokes a robust acute inflammatory response. This inflammatory reaction includes infiltration of monocytes into the vitreous and the retina, concomitant increase in expression of the proinflammatory protein, intercellular adhesion molecule 1 (ICAM-1), and death of photoreceptors. Together, these data suggest a need to further characterize the specific cellular and immune responses to the delivery of HDAd5 and develop methods to suppress these responses to improve the potential of this vector for safe large gene transfer to the retina.

MATERIALS AND METHODS

Ethics statement

Human donor eyes were collected as part of a research eye collection at the Institute for Vision Research. All samples were obtained from the Iowa Lions Eye Bank after full consent of the donors' families and in accordance with the Declaration of Helsinki. All rat experiments were conducted with the approval of the University of Iowa Animal Care and Use Committee (Animal welfare assurance No. 8051317) and were consistent with the ARVO Statement for the Use of Animals in Ophthalmic and Vision Research.

HDAd production

HDAd5 shuttle plasmids carrying either the cytomegalovirus immediate early gene promoter (CMVp) sequence upstream of enhanced green fluorescent protein (eGFP; HDAd5-CMVp-eGFP) sequence or multiple cloning site sequence (empty vector) were provided by Dr. Samuel Young and packaged at the University of Iowa Viral Vector Core Facility as described previously.[17] The University of Iowa Viral Vector Core Facility makes every effort to provide low endotoxin, sterile vectors suitable for research *in vivo* by using endotoxin-free reagents throughout the process of each batch of virus. Quality control assays for HDAd vectors include a transduced titer in plaque forming units per milliliter, a physical measure of particles per milliliter, and an assay for replication-competent adenovirus and helper virus contamination.

Culture, viral transduction, and immunohistochemistry of human retinal explants

Human donor eyes were obtained from the Iowa Lions Eye Bank (Coralville, IA) within 4–6 h of

death. The anterior segment, lens, and vitreous were removed from each eye, leaving posterior eyecups consisting of intact neural retina, choroid, and sclera. Retinal tissue was collected using a 6 mm biopsy punch and cultured in six-well transwell culture plates (Corning Life Sciences, Tewksbury, MA; Cat. No. 3412) with the photoreceptor cell layer down, as described previously.[24] For each serotype, 10 μL of AAV was injected directly beneath each of the two retinal explants, creating a bleb similar to that formed *in vivo* when performing therapeutic subretinal injections. Ten microliters of CMVp-eGFP containing HDAd5-viral particles (HDAd5-CMVp-eGFP, 5×10^{10} vector genomes [vg]) was injected directly beneath each retinal explant. An additional 10 μL of virus was added to the culture medium that was placed beneath the transwell insert (*i.e.*, 20 μL of HDAd5 was delivered per well). Explants were cultured for 7 days, with fresh media changes every 2 days.

After 7 days of culture, retinal explants were rinsed, fixed, embedded in 4% low-melting temperature agarose (Cat. No. A20070-100.0; Research Products International Corp., Mount Prospect, IL), and sectioned using a vibrating tissue slicer (Leica VT1000 S Vibratome; Leica Microsystems, Wetzlar, Germany) as described previously.[24] Sections were blocked in immunocytochemical blocking buffer for thicker sections and labeled as described previously.[25] Explant sections were labeled with the following primary antibodies: rabbit antishort wavelength (blue) cone opsin (1:1,000, Cat. No. AB5407; MilliporeSigma, Burlington, MA), rabbit antimedium, and long wavelength (green/red) cone opsins (1:1,000, Cat. No. AB5405; MilliporeSigma) and rabbit anti-PCKα (1:500, Cat. No. 2056; Cell Signaling, Danvers, MA). Sections were subsequently incubated with goat antirabbit Alexa Fluor 546 (Cat. No. A-11010; Thermo Fisher Scientific, Waltham, MA) and 4′,6-diamidino-2-phenylindole dihydrochloride (DAPI, 1:10,000; MilliporeSigma) for 2 h at room temperature in immunocytochemical blocking buffer. Sections were mounted using FluorSave Reagent (MilliporeSigma). Visualization of eGFP (driven by transduction of HDAd5) was performed without the assistance of antibody labeling. Labeled sections were visualized using a Leica TCS SPE DMi8 inverted confocal microscope system (Leica Microsystems).

Subretinal injections

Heterozygous Rowett nude (RNU) rats (Crl:NIH-*Foxn1*$^{rnu/+}$; Charles River, Wilmington, MA), hereafter referred to as RNU$^{+/-}$, have a fully functional (wild-type) immune system and were utilized in this study. Rats were anesthetized with 3–5% inhalant isoflurane (Piramal Healthcare, Bethlehem, PA), and their eyes were dilated with one to two drops of tropicamide (Alcon Laboratories, Fort Worth, TX). A limited conjunctival peritomy was created to expose the sclera, and a transscleral incision was made into the subretinal space using a 30-gauge needle. Using a blunt Hamilton syringe (Hamilton Company, Reno, NV), 10 μL of CMVp-eGFP containing HDAd5-viral particles (HDAd5-CMVp-eGFP, 5×10^{10} vg) was injected into the subretinal space. Successful subretinal injections were confirmed by the presence of a subretinal bleb assessed by fundus examination with an operating microscope and, as needed, using optical coherence tomography (OCT) (Phoenix MICRON Image-Guided OCT2; Phoenix Laboratories, Pleasanton, CA). The contralateral eye received a 10 μL subretinal injection of sterile 3% sucrose buffer as a control. Similarly, HDAd5 empty vector (HDAd5E; HDAd5-CMVp-empty), which is identical to HDAd5-CMVp-eGFP except that it lacks the eGFP transgene cassette, was titer matched and injected subretinally in the same manner. To evaluate the dose-related response to HDAd5, a 10 μL subretinal injection of HDAd5-CMVp-eGFP was performed using each of the following doses: 5×10^{9} vg ($n=4$ eyes), 5×10^{8} vg ($n=3$ eyes), and 5×10^{7} vg ($n=3$ eyes), respectively. Dose response eyes were harvested at 3 days postinjection.

Animals were sacrificed at 3 days ($n=8$; 4 males and 4 females for HDAd5 and $n=3$; 1 male and 2 females for empty vector), 7 days ($n=10$; 5 males and 5 females), and 14 days ($n=10$; 5 males and 5 females) postinjection. Before sacrifice, rat eyes were examined under an operating microscope to record clinical findings, including presence of iris synechiae (suggestive of anterior chamber inflammation), vitreous haze (consistent with posterior chamber inflammation), vascular engorgement, and chorioretinal scarring. Fundus photographs were obtained *in vivo* using the Micron III or Micron IV fundus camera with image-guided OCT (Phoenix Laboratories). A limbal suture was placed at the corresponding clock hour of the injection site for reference when embedding tissues for sectioning.

Isolation of retinal protein and Western blotting

Eyes used for protein extraction at 3 days ($n=7$; 3 males and 4 females) and 7 days ($n=7$; 5 males

and 2 females) postinjection were enucleated and immediately dissected to harvest whole retinal lysate. In brief, the cornea was dissected using Vannas scissors (Fine Science Tools, Foster City, CA) along the limbus, followed by lens removal. Each retina was carefully removed using clean microforceps (Fine Science Tools), flash-frozen in liquid nitrogen, and stored at –80°C. Whole retinas were homogenized in fresh RIPA buffer (Thermo Fisher Scientific) supplemented with cOmplete™ protease and PhosSTOP™ phosphatase inhibitor cocktails (MilliporeSigma) and lysates were cleared through tabletop microcentrifugation. Supernatant protein concentrations were determined using a BCA kit according to the manufacturer's instructions (Pierce, Rockford, IL). Western blots were performed as described previously.[8,26] Forty micrograms per sample were subjected to sodium dodecyl sulfate-polyacrylamide gel electrophoresis (SDS-PAGE; 4–20% Tris-glycine gels; Thermo Fisher Scientific), transferred to polyvinylidene difluoride using an iBlot 2 dry blotting system (Thermo Fisher Scientific), and probed with primary antibodies using an iBind Flex Western Device (Thermo Fisher Scientific). Blots were probed with the following primary antibodies: goat antimouse ICAM-1 primary antibody (1:500, Cat. No. AF796; R&D Systems, Minneapolis, MN) and mouse anti-α-tubulin (1:2,500, Cat. No. ab7291; Abcam, Cambridge, United Kingdom). The following secondary antibodies were used: donkey antigoat (1:5,000, Cat. No. A16005; Thermo Fisher Scientific) and goat antimouse (1:5,000, Cat. No. A16078; Thermo Fisher Scientific) cross-adsorbed secondary antibodies conjugated to horseradish peroxidase. Antigen–antibody complexes were visualized on X-ray film through enhanced chemiluminescence using SuperSignal West Pico PLUS (Thermo Fisher Scientific). Blots were stripped using Restore Western Blot Stripping Buffer (Thermo Fisher Scientific) and reprobed with mouse anti-α-tubulin as an internal loading control. Immunoreactivity was semiquantified using ImageJ64 (National Institutes of Health, Bethesda, MD) spot densitometry software.

Quantibody cytokine arrays

To identify key inflammatory markers for further study, some protein samples harvested at 3 days ($n=7$; 3 males and 4 females) and 7 days ($n=7$; 5 males and 2 females) postinjection were selected for Quantibody Cytokine Array (RayBiotech, Norcross, GA), a multiplex ELISA system that allows for simultaneous quantitative measurement of multiple cytokines, growth factors, and other proteins in quadruplicate. Quantibody Cytokine Arrays were performed according to manufacturer's instructions.

Immunohistochemistry and confocal microscopy

Rat eyes were enucleated, fixed in 4% paraformaldehyde overnight at 4°C, rinsed in increasing concentrations of sucrose, embedded in a 2:1 solution of Tissue-Tek OCT embedding compound (VWR International, Radnor, PA) to 20% sucrose, flash frozen in liquid nitrogen, stored at –80°C, and sectioned at a thickness of 7 μm using a Microm HM505E cryostat. Slides were blocked in immunocytochemical blocking buffer (1× phosphate-buffered saline, 3% bovine serum albumin [Research Products International Corp.], 5% normal donkey serum [Thermo Fisher Scientific], and 0.1% Tween-20 [MilliporeSigma]). Sections were labeled with the following primary antibodies: rabbit anti-Iba1 (1:1,000, Cat. No. 019-19741; Fujifilm Wako Chemicals, Richmond, VA), and goat antimouse ICAM-1 primary antibody (1:500, Cat. No. AF796; R&D Systems). Sections were subsequently incubated with goat antirabbit Alexa Fluor 546 (Cat. No. A-11010; Thermo Fisher Scientific) and donkey antigoat Alexa Fluor 647 (Cat. No. A-21447; Thermo Fisher Scientific) secondary antibodies and DAPI (1:10,000; MilliporeSigma) for 2 h at room temperature in immunocytochemical blocking buffer. Sections were mounted using FluorSave Reagent (MilliporeSigma). Visualization of eGFP (driven by transduction of HDAd5) was performed without the assistance of antibody labeling. Labeled sections were visualized using a Leica TCS SPE DMi8 inverted confocal microscope system (Leica Microsystems). Each specific marker was investigated in the following manner: three nonoverlapping images were acquired per section from each of two nonserial sections per slide (*i.e.*, with four serial sections per slide, sections immediately adjacent one another were never imaged) on a minimum of three nonadjacent slides per eye. This approach ensured that images or data from the same eye were never duplicated. Representative images are shown.

Statistical analysis

A paired two-tailed Student's *t*-test was performed to determine significance between ICAM-1 protein levels through Western blotting in HDAd5-CMVp-eGFP versus sucrose buffer-injected contralateral control eyes using Prism 6 (Graphpad Software, La Jolla, CA). $p<0.05$ was considered statistically significant.

RESULTS

HDAd5-CMVp-eGFP transduces human photoreceptors

As HDAds have been shown to efficiently transduce and mediate long-term transgene expression within postmitotic retinal neurons of mice,[18,19] they are promising candidates for delivery of large retinal genes. However, the degree of photoreceptor tropism is unclear from published studies.[18,19] Therefore, we first tested HDAd5-CMVp-eGFP (Fig. 1A) retinal tropism in *ex vivo* organ cultures of human donor retina. We previously demonstrated this approach as a useful method for evaluating the transduction efficiency and retinal tropism of different AAV serotypes.[24] HDAd5-driven eGFP expression was observed throughout the neural retina of human explants, including the outer nuclear layer and rod and cone photoreceptors (Fig. 1B, C), demonstrating HDAd5's potential as a vector for delivery of large retinal disease-causing genes.

Subretinal injection of HDAd5 induces pigmentary and vascular changes in the retina

Although HDAds possess several attractive properties for large gene delivery, after injection, tissue-specific reactions need to be evaluated before clinical application. For instance, although prior studies of HDAds delivered subretinally in mice did not detect an associated immune response,[18,19] studies evaluating delivery of HDAds to mouse lung and liver have demonstrated a strong acute inflammatory reaction.[21,22] To determine whether HDAd5 (a commonly used serotype that has been shown to effectively transduce the retina in mice[19]) is tolerated by the immune system, we injected 10 μL of either HDAd5-CMVp-eGFP (5×10^{10} vg for a total of 5×10^{8} g/injection) or 3% sterile sucrose buffer into the subretinal space of immune competent rats. At 3 days postinjection, eyes injected with HDAd5 possessed posterior iris synechiae, moderate vitreous haze, and vascular engorgement, and sheathing, suggestive of an acute panuveitis (Fig. 2A). In contrast, sucrose buffer-injected contralateral control eyes were completely quiet at the same time point (Fig. 2D). The vitreous haze persisted at 7 days postinjection (Fig. 2E vs. H) and led to severe chorioretinal pigmentary changes, and atrophy at 7 and 14 days postinjection (Fig. 2E, I, white asterisks) compared with buffer-injected eyes at the same time points (Fig. 2H, L). Strong eGFP-positive reporter expression around the injection site was observed at each of the three time points assessed: 3, 7, and 14 days post-HDAd5 injection (Fig. 2B, F, J), as demonstrated in overlay images with color fundus photos (Fig. 2C, G, K).

Exposure to HDAd5 induces vitreoretinal inflammation

To better characterize the eGFP expression seen on fluorescent fundus photographs and evaluate the extent of eGFP expression, we acquired confocal fluorescent images at 3 days postinjection. A representative panoramic confocal fluorescent image is shown (Fig. 3A). There was robust eGFP expression in the retinal pigmented epithelium (RPE), as well as some eGFP-positive signal throughout the neural retina (Fig. 3A, 3A' and 3A"), confirming successful and accurate subretinal delivery of HDAd5-CMVp-eGFP with transduction of multiple retinal layers.

We observed clinical evidence of inflammation (*e.g.*, iris synechiae formation, vitreous haze, retinal vascular engorgement, and chorioretinal pigmentary changes) at 3 days postinjection,

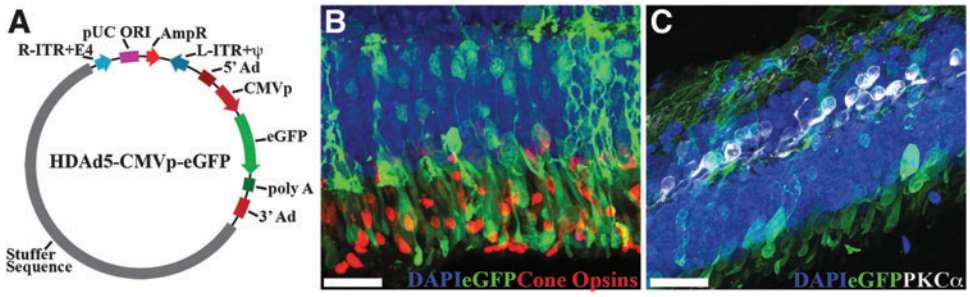

Figure 1. HDAd5-CMVp-eGFP transduces human photoreceptors. **(A)** Schematic depicting HDAd5-CMVp-eGFP vector plasmid. R-ITR+E4, right-inverted terminal repeat+E4 portion of adenovirus gene; pUC ORI, pUC plasmid origin of replication; AmpR, ampicillin resistance cassette; L-ITR-Ψ, left-inverted terminal repeat+packaging signal; 5′Ad, 5′ adenovirus sequence; CMVp, cytomegalovirus promoter; eGFP, enhanced green fluorescent protein; poly A, polyadenylation; 3′ Ad, 3′ adenovirus sequence. **(B, C)** Confocal micrographs showing HDAd5-driven eGFP (*green*) expression in human retinal explants and immunohistochemical labeling with anticone opsins **(B;** *red***)** and anti-PKCα **(C;** *white***)** antibodies. Retinal nuclei were counterstained with DAPI (*blue*). Scale bars = 50 μm. DAPI, 4′,6-diamidino-2-phenylindole dihydrochloride; HDAd, helper-dependent adenoviruses.

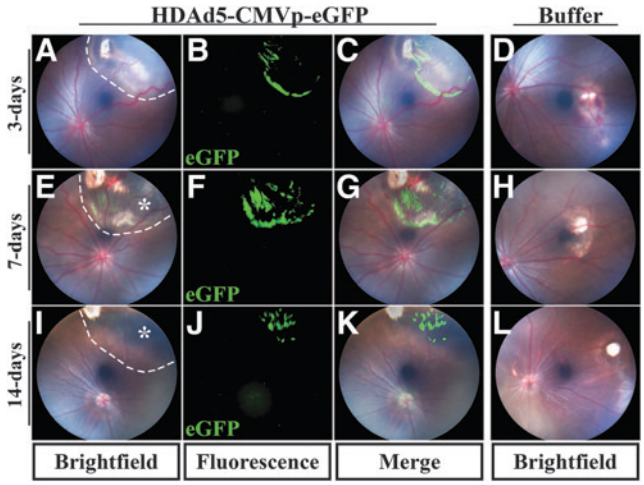

Figure 2. Subretinal injection of HDAd5-CMVp-eGFP induces atrophic chorioretinal scarring in rat eyes. **(A–L)** Representative bright field color fundus and eGFP-positive fluorescent images at 3 days **(A–C)**, 7 days **(E–G),** or 14 days **(I–K)** postinjection of HDAd5-CMVp-eGFP virus. Representative bright field color fundus images of sucrose buffer-injected contralateral control eyes are also shown at 3 days **(D)**, 7 days **(H),** and 14 days **(L)** postinjection. Merged images of color fundus and eGFP fluorescence for HDAd5-injected eyes are shown in **(C)**, **(G),** and **(K)**. *Dotted lines* demarcate the boundary of each subretinal injection bleb in **(A)**, **(E),** and **(I)**. *Asterisks* in **(E)** and **(I)** denote chorioretinal pigmentary atrophic changes. eGFP, enhanced green fluorescent protein.

consistent with an acute inflammatory response to subretinal injection of HDAd5. As a hypothesis-generating experiment to guide our further characterization of this inflammation, we identified a subset of inflammatory markers involved in the response to HDAd5 using multiplex cytokine arrays on whole vitreoretinal protein lysates isolated from HDAd5- and sucrose buffer-injected eyes at 3 and 7 days postinjection. Although data derived from multiplex arrays are inherently widespread, a consistent increase was observed in multiple proinflammatory markers, including monocyte chemoattractant protein 1 or chemokine (C-C motif) ligand 2 (MCP-1/CCL2), L-selectin, and ICAM-1 (data not shown). These proteins are involved in the chemotaxis and transmigration of circulating monocytes from the blood into tissues.[27,28] Based on these cytokine array results and the clinical findings, we hypothesized that subretinal injection of HDAd5 is driving an inflammatory response that includes the infiltration of cells into the vitreous and neural retina.

To characterize the cellular infiltration, we next labeled retinal sections with anti-Iba1 antibody (formerly known as allograft inflammatory factor 1), a known marker of resident retinal microglia, as well as circulating monocytes, including macrophages,[29,30] and again constructed fluorescent panoramic images to represent an entire cross-section of the posterior pole from both buffer- and HDAd5-injected eyes (Fig. 3B, C) at 3 days postinjection. Compared with control buffer-injected eyes (Fig. 3B, B'), HDAd5 induced a marked infiltration of Iba1-positive cells into the vitreous that spanned the entirety of the posterior pole (Fig. 3C, white asterisk). Higher magnification

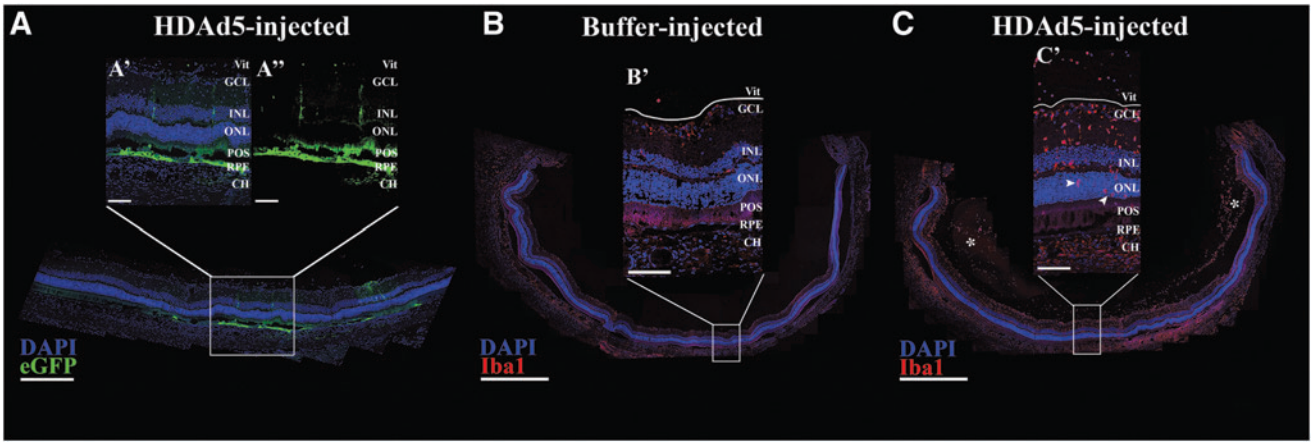

Figure 3. Subretinal injection of HDAd5-CMVp-eGFP induces cellular infiltration into the vitreous by 3 days postinjection. **(A)** Representative ($n=8$; 4 males and 4 females, injected in two independent cohorts) panoramic confocal image depicting site of injection of HDAd5-CMVp-eGFP (eGFP; *green*) at 3 days postinjection. Transduction and eGFP expression are observed in the RPE and throughout the neural retina **(A', A'')**. DAPI (*blue*) was used to counterstain cell nuclei. **(B, C)** Panoramic confocal images displaying an entire section through a buffer-injected **(B, B')** and an HDAd5-injected **(C, C')** eye at 3 days postinjection labeled with Iba1 (*red*) and the nuclear counterstain, DAPI (*blue*). *White asterisks* in **(C)** denote large clusters of vitreous cells, and *white arrowheads* **(C')** point to the presence of Iba1-positive cells within the outer nuclear layer in a vector-treated eye. The *solid white line* in each *inset* demarcates the boundary between the GCL and the vitreous (Vit). Scale bars: **(A)** 400 μm, **(A', A'')** 100 μm, **(B, C)** 1000 μm, and **(B' C')** 100 μm. CH, choroid; Iba1, ionized calcium-binding adapter molecule 1; GCL, ganglion cell layer; INL, inner nuclear layer; ONL, outer nuclear layer; POS, photoreceptor outer segments; RPE, retinal pigmented epithelium.

images reveled that Iba1-positive cells were present throughout each layer of the neural retina (Fig. 3C, 3C'). Under normal conditions, Iba1-positive resident retinal microglia are typically found within the inner plexiform layer (*i.e.*, between the ganglion cell layer and inner nuclear layer[31]) and the outer plexiform layer (*i.e.*, between the inner and outer nuclear layers[31]), consistent with what we observed in sucrose buffer-injected control eyes (Figs. 3B, B' and Fig. 4A). Strikingly, Iba1-positive cells were even observed within the outer nuclear layer, which is normally composed of only the photoreceptor cell nuclei (Fig. 3C', white arrowheads and Fig. 4B). Based on the results of the cytokine array, we evaluated the expression of the proinflammatory adhesion molecule, ICAM-1, through immunohistochemistry and found that Iba1-positive infiltrates also expressed ICAM-1 (Fig. 4B). Immunoblotting of whole vitreoretinal protein lysates also confirmed a significant increase in total ICAM-1 protein at 3 days postinjection (Fig. 4C).

We next assessed the eGFP expression pattern and labeling with anti-Iba1 and anti-ICAM-1 antibodies at 7 days postinjection. Figure 5 shows retinas from three independently injected animals side-by-side, demonstrating the consistency of both our subretinal delivery and the inflammatory response to HDAd5 compared with a sucrose buffer-injected control eye. eGFP-positive signal was consistently observed within the RPE layer and throughout the neural retina, including photoreceptors. By 7 days postinjection, most Iba1-positive cells had migrated from the vitreous into the neural retina, taking residence throughout each layer, including the outer nuclear layer (Fig. 5J–L). The majority of Iba1-positive cells were also positively labeled with anti-ICAM-1 antibody (Fig. 5N–P), and total ICAM-1 protein remained significantly increased at 7 days postinjection in HDAd5-treated eyes compared with buffer-injected control eyes (Fig. 5U). Together, these data indicate that subretinal injection of HDAd5-CMVp-eGFP provokes a robust acute vitreoretinal inflammatory response involving Iba1 and ICAM-1–positive cells.

The inflammatory response to HDAd5 leads to loss of photoreceptor cells

At 14 days postinjection, HDAd5-mediated eGFP expression was still observed throughout the neural retina but was minimal in the outer nuclear layer (Fig. 6F, H) and RPE (Fig. 6F). A large population of Iba1-positive cells persisted throughout the retina of HDAd5-injected eyes compared with buffer-injected controls (Fig. 6C vs. G), and there was noticeable thinning of the outer nuclear layer in vector-treated eyes, consistent with photoreceptor cell death (Fig. 6A, D vs. 6E, H). Despite the outer retinal loss, the inner retina, including inner nuclear layer, appeared similarly preserved in both buffer- and HDAd5-treated eyes.

The inflammatory response is to the HDAd5 vector and not overexpression cytotoxicity

As shown in previous figures, injection of sterile sucrose buffer resulted in minimal inflammation or cellular loss relative to the those injected with HDAd5, suggestive of minimal injury from the subretinal injection itself. However, to demonstrate

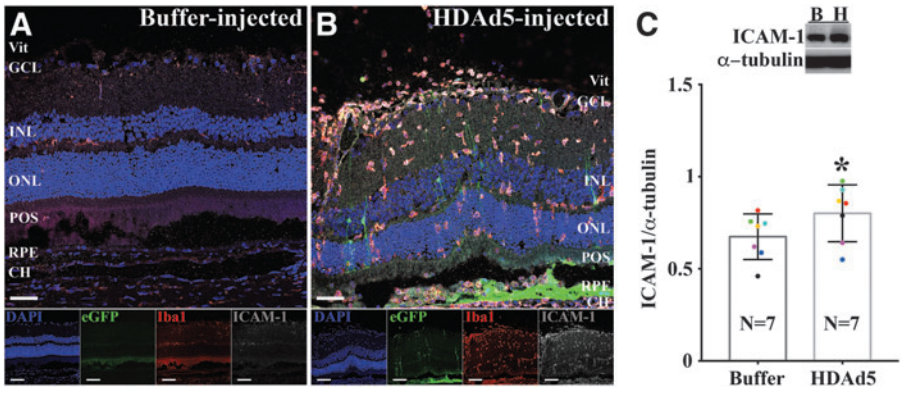

Figure 4. HDAd5-induced inflammatory infiltrates express ICAM-1. **(A, B)** Representative ($n=8$; 4 males and 4 females, injected in two independent cohorts) fluorescent confocal micrographs of a buffer- **(A)** and HDAd5-injected **(B)** eye demonstrating expression of eGFP (*green*) and labeled with anti-Iba1 (*red*) and anti-ICAM-1 (*gray*). Cell nuclei were counterstained with DAPI (*blue*). Individual fluorophores are shown below each merged image. Scale bars = 100 μm in each image and definition of abbreviations is same as in Fig. 3. **(C)** Representative Western blot ($n=7$) comparing protein levels of ICAM-1in buffer-injected (*lane B*) and HDAd5-injected (*lane H*) whole vitreous/retinal lysates at 3 days postinjection. α-tubulin was used as a loading control. Semiquantitative comparison between buffer- and vector-injected eyes shows a statistically significant increase (*) in ICAM-1 expression ($p<0.05$). *Like-colored dots* represent contralateral eyes from the same animal. ICAM-1, intercellular adhesion molecule 1.

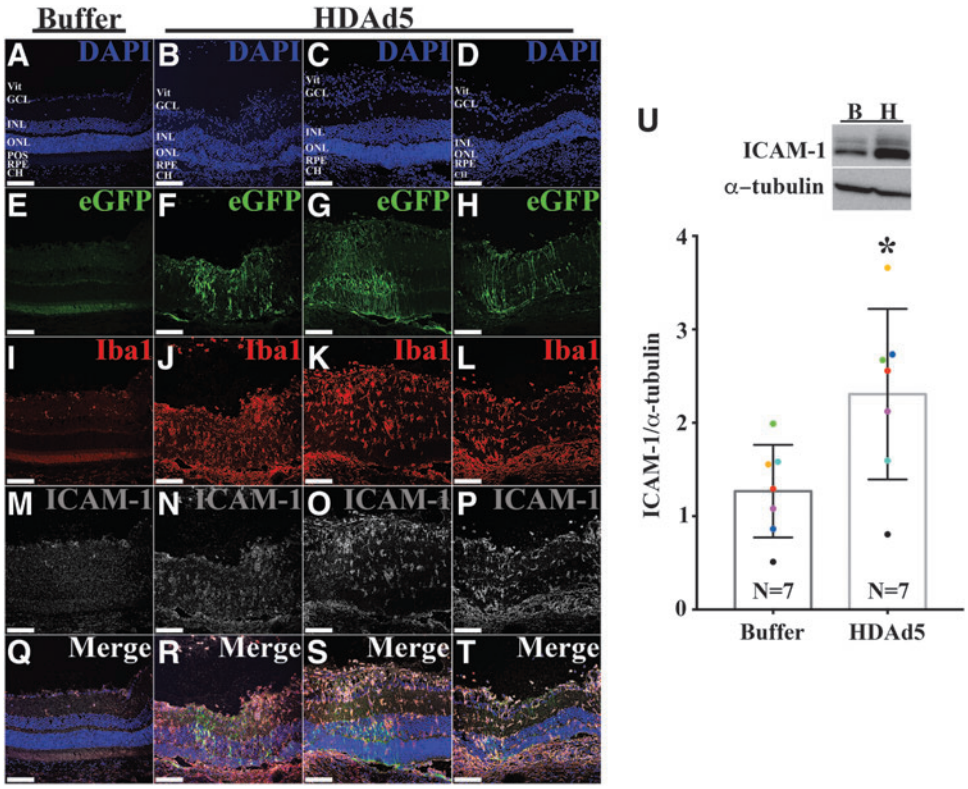

Figure 5. By 7 days postinjection of HDAd5, most vitreous cell infiltrates have migrated into the neural retina. **(A–T)** Representative ($n=10$; 5 males and 5 females) confocal fluorescent images comparing a buffer-injected eye **(A, E, I, M, Q)** to three independent eyes given HDAd5-CMVp-eGFP **(B, F, J, N** and **R**; **C, G, K, O** and **S; D, H, L, P,** and **T)** at 7 days postinjection. Transduction of HDAd5 induces expression of eGFP **(***green*; **F–H)** compared with a buffer-injected control eye **(E)**. Sections are also labeled with anti-Iba1 **(***red*; **I–L)**, anti-ICAM-1 **(***gray*; **M–P),** and the nuclear counterstain, DAPI **(***blue*; **A–D)**. Merged images for each eye are shown in **(Q–T)**. Definition of abbreviations is same as in Fig. 3. Scale bars = 100 μm in each image. **(U)** Representative Western blot ($n=7$) comparing protein levels of ICAM-1 in buffer-injected (*lane B*) and HDAd5-injected (*lane H*) whole vitreous/retinal lysates at 7 days postinjection. α-tubulin was used as a loading control. Semiquantitative comparison between buffer- and vector-injected eyes shows a statistically significant (*) in ICAM-1 expression ($p<0.05$). *Colored dots* represent contralateral eyes from the same animal.

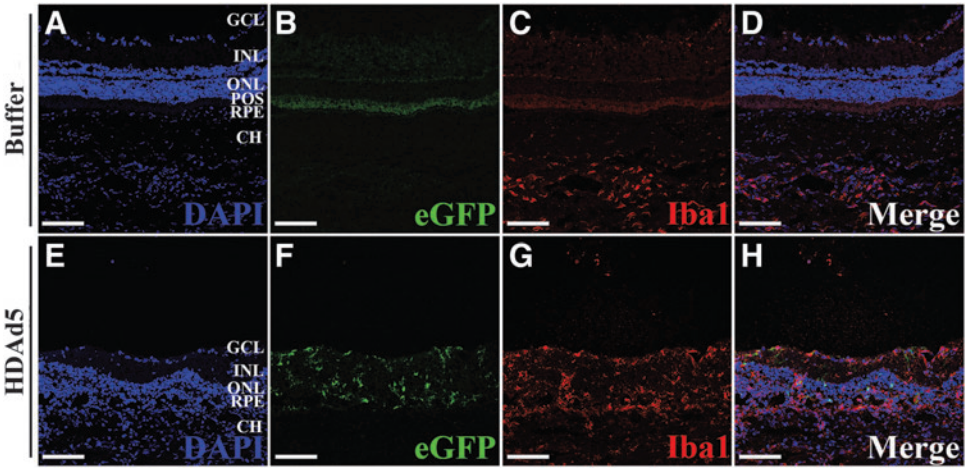

Figure 6. The inflammatory response to HDAd5 leads to death of photoreceptors and thinning of the outer nuclear layer. Representative ($n=10$; 5 males and 5 females) fluorescent confocal microscopic images of buffer- and HDAd5-injected eyes at 14 days after injection. Sections were counterstained with DAPI to label nuclei **(***blue*; **A, E)** and labeled with anti-Iba1 **(***red*; **C, G)**. eGFP **(***green*; **B, F)** was also assessed and only expressed in HDAd5-injected eyes. Merged images for buffer- and HDAd5-injected are shown in **(D)** and **(H)**, respectively. Definition of abbreviations is same as in Fig. 3. Scale bars = 100 μm in each image.

that the inflammation and eventual photoreceptor cell loss seen in HDAd5-CMVp-eGFP-injected eyes were not due to cytotoxic overexpression of GFP,[32] we repeated injections using an empty HDAd5 vector that contained all of the same elements as HDAd5-CMVp-eGFP (Fig. 1A) except the eGFP transgene cassette (HDAd5E). We performed subretinal injections of titer-matched viruses in independent animals wherein only one eye received HDAd5E. In the absence of an eGFP transgene and eventual green fluorescent signal to localize the distribution of the subretinal bleb, we performed OCT imaging immediately after injection of HDAd5E to confirm successful subretinal delivery (Fig. 7A, B). Importantly, at 3 days postinjection, HDAd5E provoked an identical inflammatory

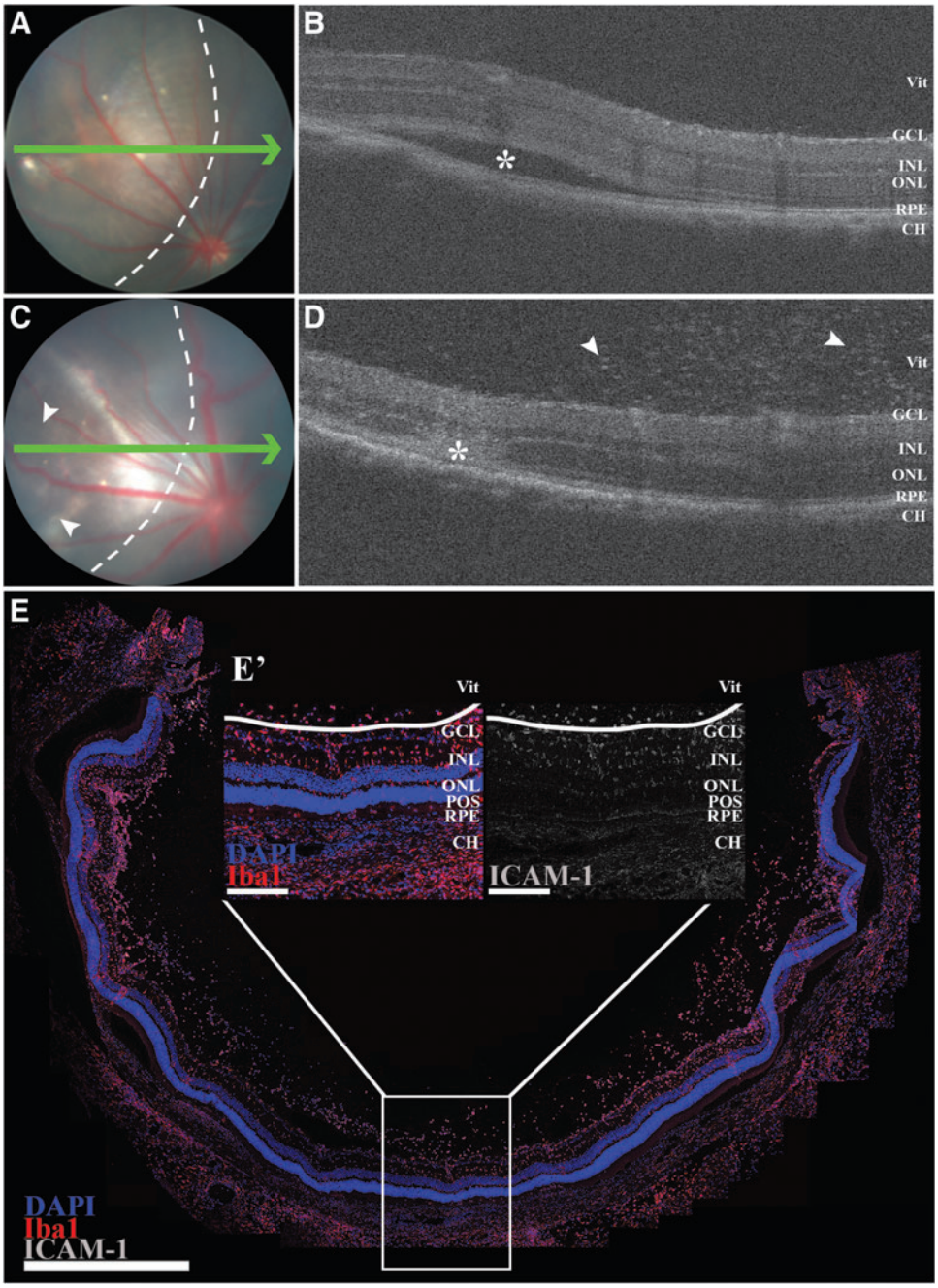

Figure 7. The inflammatory response to HDAd5 is present using an empty vector that does not drive expression of eGFP. Fundus images **(A, C)** and OCT scans **(B, D)** immediately after **(A, B)** and 3 days **(C, D)** postsubretinal injection of HDAd5E in the same eye. *Green arrows* in **(A)** and **(C)** correspond to location of each OCT line scan. *Dotted lines* in **(A)** and **(C)** denote margin of injection bleb. *Asterisk* in **(B)** demarcates subretinal bleb created by injection and *asterisk* in **(D)** marks the site of injection after bleb resolution 3 days postinjection. *White arrowheads* in **(D)** point to vitreous cell infiltrates. **(E)** Representative panoramic confocal image displaying an entire section through an HDAd5E-injected **(E')** eye at 3 days postinjection. OCT, optical coherence tomography.

response compared with HDAd5-CMVp-eGFP, including the presence of vitreous cell infiltrates as shown through OCT (Fig. 7C, D), and immunohistochemical labeling with anti-Iba1 and anti-ICAM-1 antibodies (Fig. 7E) demonstrates that the observed findings are in response to the HDAd5 vector and not due to eGFP-mediated overexpression cytotoxicity.

The inflammatory response to HDAd5 vector is dose dependent

To assess whether the observed acute inflammatory response to HDAd5-CMVp-eGFP is related to the dose (*i.e.*, 5×10^{10} vg) being administered, we performed a dose–response experiment comparing three additional doses at three lower log-unit increments: 5×10^{9}, 5×10^{8}, and 5×10^{7} vg. We injected each dose into the subretinal space in the same manner as for the high dose (5×10^{10} vg) experiments and performed immunohistochemistry using anti-Iba1 and anti-ICAM-1 antibodies at 3 days postinjection to assess the level of inflammation and cellular infiltration. As shown in Fig. 8, the inflammatory response to 5×10^{9} was very similar to that observed with the higher dose (5×10^{10} vg) demonstrated throughout the article. Importantly, at this lower dose, the amount of eGFP expression in the neural retina was noticeably less, suggesting that retinal transduction is dose dependent. Decreasing the dose by another log unit (*i.e.*, 5×10^{8}) decreased the amount of Iba1-positive cellular infiltrates but produced even less eGFP signal, which was only observed in the RPE (*i.e.*, minimal-to-no signal in the neural retina). Finally, injection of the lowest dose of 5×10^{7} completely ameliorated cellular infiltration, but also resulted in no observed eGFP fluorescence in the retina or RPE.

DISCUSSION

This study demonstrates that HDAd5 effectively transduces the human retina, including photoreceptors, supporting the potential of HDAd5 as a vector for large gene replacement therapy. However, *in vivo* subretinal injection of HDAd5 elicits a robust inflammatory response in the rat, emphasizing that the development of any gene therapy will require strategies for mitigating immune-mediated injury. The acute innate response in rat includes vitreoretinal infiltration of monocytes and increased expression of the inflammatory protein ICAM-1. Although the inflammatory response is dampened when lower doses are administered, this reduction in inflammation comes at the cost of lower retinal transduction, which could mitigate any potential efficacy from gene replacement. Further characterization of the immune response

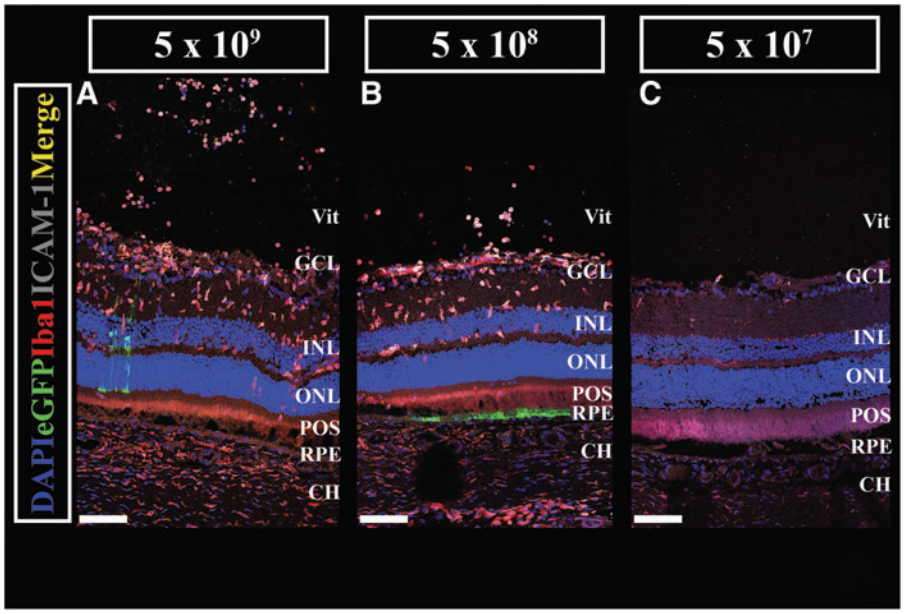

Figure 8. Decreasing the dose of HDAd5-CMVp-eGFP by 3 log units abrogates inflammatory cellular infiltration, but also yields no visible retinal transduction. **(A–C)** Representative ($n=3$ eyes injected per dose) confocal images at 3 days postinjection near the site of injection of HDAd5-CMVp-eGFP (eGFP; *green*) at each of three different doses: 5×10^{9} vg **(A)**, 5×10^{8} vg **(B)**, and 5×10^{7} vg **(C)**. Each image is labeled with anti-Iba1 (*red*), anti-ICAM-1 (*gray*), and the nuclear counterstain, DAPI (*blue*). Scale bars = 100 μm. Definition of abbreviations for retinal layers is the same as Fig. 3.

will be important for developing safe and effective large-gene replacement therapy using HDAd5.

Although HDAd5 has previously been shown to transduce the neural retina in mice, the degree of photoreceptor tropism is unclear from these studies.[18,19] Therefore, to explore its potential for use in human subjects, we first confirmed HDAd5 photoreceptor tropism in human donor retinal explants. We previously demonstrated the utility of this approach by testing the retinal transduction efficiency and tropism of seven different AAV serotypes.[24] As shown in Figs. 3–6, the tropism of HDAd5 is patchy and, for the most part, does not appear to transduce retinal photoreceptors in rat, likely due to fundamental species differences between humans and rats. As the inflammatory or immune response to HDAd5 cannot be assessed preclinically in humans, we chose rat as a mechanism for evaluating the immune response to subretinal injection of HDAd5.

HDAds are a "gutless" version of first-generation adenoviruses that lack viral coding regions, affording HDAds a larger packaging capacity than first-generation adenoviruses. First-generation adenoviruses evoke an inflammatory and immune response that typically involves both nonspecific innate and adaptive mechanisms and occurs in three distinct phases.[21] First, an immediate acute phase is triggered within minutes of administration, involving an inflammatory response to the adenovirus capsid proteins, including upregulation of proinflammatory cytokines and chemokines and activation of immune effector cells such as macrophages. Second, an intermediate phase takes place within a few hours to a day that involves monocyte migration, activation, and infiltration. Finally, a late phase occurs over a time period of days to several weeks that includes an adaptive immune response triggered by an uptake of adenoviral particles by antigen presenting cells and downstream activation of cytotoxic T cells.[21] The absence of viral genes theoretically dampens the host adaptive immune response to HDAds.[22] However, because the initial inflammatory and nonspecific innate immune responses are induced by presence of viral capsid proteins, HDAds still incite an acute and intermediate phase inflammatory response after subretinal injections in rats, similar to that previously reported after delivery in the liver and lung of mice.[22,33]

A severe immune response is potentially harmful regardless of the target tissue receiving treatment. However, an inflammatory response like that described in this study could potentially have more severe consequences in the neural retina, which is almost entirely composed of postmitotic terminally differentiated neurons (*i.e.*, the mammalian retina has little to no capacity for self-renewal) compared with the liver, which possesses regenerative capacity in response to damage.[34,35] Indeed, we observed that at 2 weeks after subretinal delivery, the HDAd5-mediated response led to loss of the outer nuclear layer, indicative of photoreceptor cell death. Vector-associated damage to the photoreceptors would severely limit the utility of HDAd5 for the treatment of inherited retinal diseases, the majority of which are photoreceptor diseases wherein the patient may have little retinal tissue in reserve.[7] In a normal eye, the blood–retinal barrier typically acts to sequester the neural retina from the surrounding immune system.[36,37] However, in retinal degenerative diseases that involve the loss of RPE and/or photoreceptors, the subretinal space becomes a proinflammatory environment.[38,39] As such, the observed HDAd5-mediated response would likely be enhanced if administered to a retinal degenerative eye wherein the integrity of the blood–retinal barrier is already compromised.

Preclinical experiments like that described here are important when considering a vector for potential therapeutic use, and the early identification of potentially harmful inflammatory complications provides an opportunity to address these aspects before proceeding to human clinical trials. For example, Reichel *et al.* demonstrated that subretinal injection of AAV8 elicited both an innate and adaptive immune response in primates, triggering infiltration of Iba1- and CD8-positive cells, respectively.[40] Similarly, Marangoni *et al.* reported inflammatory cell infiltrates in the vitreous of New Zealand White rabbits after intravitreal delivery of AAV8 coding the human retinoschisin protein.[41] Despite these observations, a phase I/IIa clinical dose-escalation trial (NCT02317887) was conducted to evaluate the safety and efficacy of AAV8-*RS1* in nine patients with molecularly confirmed *RS1* X-linked retinoschisis.[5] Cukras *et al.* reported that the virus was well tolerated in all but one of the individuals, but they also observed dose-dependent inflammation, including an increase in systemic antibodies raised against the AAV8 capsid.[5] Although the authors suggest that these inflammatory events can be managed using topical and oral steroids, this study raises the question of whether additional doses of virus or different means of immunosuppression should be pursued to optimize the safety of AAV8-mediated delivery in the retina.

Armed with the knowledge gained from this study that subretinal delivery of HDAd5 elicits a

strong inflammatory response, we now have the opportunity to fully characterize the mechanism of this inflammatory response (*i.e.*, the infiltration of Iba1-positive monocytes) and address the question of whether there is a later onset adaptive immune response. In this study, we chose to test the immune response to HDAd5 in the $RNU^{+/-}$ rat model, which possesses a fully intact immune system. Future experiments utilizing the RNU homozygous genetic rat line (Crl:NIH-*Foxn1*$^{rnu/rnu}$ or $RNU^{-/-}$), which are athymic (*i.e.*, lack T cells) and cannot mount an adaptive immune response, would help determine the degree to which the adaptive arm of the immune system is involved in the response to HDAd5. Furthermore, several groups have demonstrated that pharmacological depletion of macrophages attenuates the innate immune response to adenoviruses.[42,43] Thus, combining genetic and pharmacological approaches will allow for the identification of the specific molecular and cellular mechanisms driving the immune response to HDAd5. Moreover, elucidation of these mechanisms will help determine the best mode in which to test the extent that immunosuppression can mitigate the harmful response to HDAd5 in the retina.

This study does have a number of limitations. For example, an unanswered question is whether the rats used in this study were previously exposed to adenovirus 5 from the environment, which would greatly affect the adaptive immune response to the viral capsid. However, inbred rats housed in a barrier facility are unlikely to have been exposed to this specific virus. In contrast, most humans have been exposed to adenovirus 5 and, therefore, have already raised system-neutralizing antibodies against the virus,[44,45] which could exacerbate the immune response to HDAd5 and potentially decrease the transduction efficiency due to the clearance of HDAd5-infected cells. Although we observed robust HDAd5-mediated eGFP fluorescence within the RPE and throughout the neural retina, the observed transduction was patchy, and we did not quantify the transduction efficiency in distinct layers of the retina. However, as others have also demonstrated, HDAd5 did not appear to target photoreceptors as efficiently as the RPE and inner retina.[18,19] One possibility for the limited number of eGFP-positive photoreceptors is that these cells, once transduced, may be specifically targeted for early phagocytosis by either activated resident microglia or infiltrating Iba1-positive monocytes. It is also possible that HDAd5-CMVp-eGFP does not efficiently transduce photoreceptors, in which case, an option to improve targeting of photoreceptors may be to engineer an HDAd5 with a photoreceptor-specific promoter such as rhodopsin[46] or rhodopsin kinase[47] instead of the stronger constitutively active cytomegalovirus promoter.

Importantly, we demonstrated that the observed infiltration of inflammatory cells is a response to the HDAd5 vector and not a result of overexpression cytotoxicity due to delivery of eGFP. But, what would be the consequences of overexpressing a large retinal cDNA like *ABCA4*, which needs to be correctly folded and transported to a specific area of the photoreceptor outer segment? Several groups have reported that overexpression of opsins alters photoreceptor structure, decreases light response by photoreceptors, and induces photoreceptor degeneration.[48,49] Moreover, we have previously shown that overexpression of *CEP290* driven by the CMV promoter induces overexpression cytotoxicity and cell death in mouse-induced pluripotent stem cell-derived photoreceptor precursor cells.[8] Overexpression cytotoxicity represents another hurdle that will likely need to be overcome for safe and effective delivery of at least some large retinal cDNAs.

HDAds transduce the retina and hold promise for retinal gene replacement therapy, particularly those caused by genes too large for packaging into an AAV. This study is the first to explore the delivery of HDAds to the rat retina and demonstrates that subretinal injection of HDAd5 elicits a strong inflammatory cellular response independent of eGFP overexpression. Future studies will focus on characterizing the specific cell types involved in the vitreoretinal infiltration as well as the molecular signals responsible for driving this acute response. It is yet unknown whether panimmunosuppression or targeted local immunosuppression will be able to attenuate this response sufficiently to make delivery of large retina cDNAs feasible, and future studies will evaluate the effect of various modes of immunosuppression on the HDAd-associated inflammatory response. The identification of the components of the immune response to HDAd5 will facilitate the development of combinatorial therapy directed at increasing the maximal tolerated dose of subretinally delivered adenoviral vectors and may eventually allow vectors of this type to be used for the safe delivery of large retinal genes.

ACKNOWLEDGMENTS

The authors gratefully thank the Iowa Lions Eye Bank for its continued support of vision research and also thank Dr. Chunhua Jiao, Miss Gabby Thomsen, Miss Katie Sheehan, and Mr. Emilio

Tovar for their efforts in acquiring cryosections of rat eye tissue.

AUTHOR DISCLOSURE

No competing financial interests exist for any of the authors of this article.

FUNDING INFORMATION

This study was supported by The University of Iowa Institute for Vision Research, Research of Prevent Blindness, and National Institutes of Health Grant (NIH; Bethesda, MD, USA): P30 EY025580.

REFERENCES

1. Bainbridge JW, Smith AJ, Barker SS, et al. Effect of gene therapy on visual function in Leber's congenital amaurosis. N Engl J Med 2008;358: 2231–2239.
2. Bainbridge JW, Mehat MS, Sundaram V, et al. Long-term effect of gene therapy on Leber's congenital amaurosis. N Engl J Med 2015;372: 1887–1897.
3. Russell S, Bennett J, Wellman JA, et al. Efficacy and safety of voretigene neparvovec (AAV2-hRPE65v2) in patients with RPE65-mediated inherited retinal dystrophy: a randomised, controlled, open-label, phase 3 trial. Lancet 2017;390: 849–860.
4. Dimopoulos IS, Hoang SC, Radziwon A, et al. Two-year results after AAV2-mediated gene therapy for choroideremia: the Alberta experience. Am J Ophthalmol 2018;193:130–142.
5. Cukras C, Wiley HE, Jeffrey BG, et al. Retinal AAV8-RS1 gene therapy for X-linked retinoschisis: initial findings from a phase I/IIa trial by intravitreal delivery. Mol Ther 2018;26:2282–2294.
6. Balaggan KS, Ali RR. Ocular gene delivery using lentiviral vectors. Gene Ther 2012;19:145–153.
7. Stone EM, Andorf JL, Whitmore SS, et al. Clinically focused molecular investigation of 1000 consecutive families with inherited retinal disease. Ophthalmology 2017;124:1314–1331.
8. Burnight ER, Wiley LA, Drack AV, et al. CEP290 gene transfer rescues Leber congenital amaurosis cellular phenotype. Gene Ther 2014;21:662–672.
9. Binley K, Widdowson P, Loader J, et al. Transduction of photoreceptors with equine infectious anemia virus lentiviral vectors: safety and biodistribution of StarGen for Stargardt disease. Invest Ophthalmol Vis Sci 2013;54:4061–4071.
10. Zallocchi M, Binley K, Lad Y, et al. EIAV-based retinal gene therapy in the shaker1 mouse model for usher syndrome type 1B: development of UshStat. PLoS One 2014;9:e94272.
11. Campochiaro PA, Lauer AK, Sohn EH, et al. Lentiviral vector gene transfer of endostatin/angiostatin for macular degeneration (GEM) study. Hum Gene Ther 2017;28:99–111.
12. Balaggan KS, Binley K, Esapa M, et al. Stable and efficient intraocular gene transfer using pseudotyped EIAV lentiviral vectors. J Gene Med 2006;8: 275–285.
13. Calame M, Cachafeiro M, Philippe S, et al. Retinal degeneration progression changes lentiviral vector cell targeting in the retina. PLoS One 2011;6: e23782.
14. Hacein-Bey-Abina S, Von Kalle C, Schmidt M, et al. LMO2-associated clonal T cell proliferation in two patients after gene therapy for SCID-X1. Science 2003;302:415–419.
15. Hacein-Bey-Abina S, von Kalle C, Schmidt M, et al. A serious adverse event after successful gene therapy for X-linked severe combined immunodeficiency. N Engl J Med 2003;348:255–256.
16. Cots D, Bosch A, Chillon M. Helper dependent adenovirus vectors: progress and future prospects. Curr Gene Ther 2013;13:370–381.
17. Montesinos MS, Satterfield R, Young SM, Jr. Helper-dependent adenoviral vectors and their use for neuroscience applications. Methods Mol Biol 2016;1474:73–90.
18. Lam S, Cao H, Wu J, et al. Highly efficient retinal gene delivery with helper-dependent adenoviral vectors. Genes Dis 2014;1:227–237.
19. Puppo A, Cesi G, Marrocco E, et al. Retinal transduction profiles by high-capacity viral vectors. Gene Ther 2014;21:855–865.
20. Persson A, Fan X, Widegren B, et al. Cell type- and region-dependent coxsackie adenovirus receptor expression in the central nervous system. J Neurooncol 2006;78:1–6.
21. Seiler MP, Cerullo V, Lee B. Immune response to helper dependent adenoviral mediated liver gene therapy: challenges and prospects. Curr Gene Ther 2007;7:297–305.
22. Muruve DA, Cotter MJ, Zaiss AK, et al. Helper-dependent adenovirus vectors elicit intact innate but attenuated adaptive host immune responses in vivo. J Virol 2004;78:5966–5972.
23. Piccolo P, Brunetti-Pierri N. Challenges and prospects for helper-dependent adenoviral vector-mediated gene therapy. Biomedicines 2014;2: 132–148.
24. Wiley LA, Burnight ER, Kaalberg EE, et al. Assessment of adeno-associated virus serotype tropism in human retinal explants. Hum Gene Ther 2018;29:424–436.
25. Wiley LA, Beebe DC, Mullins RF, et al. A method for sectioning and immunohistochemical analysis of stem cell-derived 3-D organoids. Curr Protoc Stem Cell Biol 2016;37:1C 19 11–11C 19 11.
26. Burnight ER, Gupta M, Wiley LA, et al. Using CRISPR-Cas9 to generate gene-corrected autologous iPSCs for the treatment of inherited retinal degeneration. Mol Ther 2017;25:1999–2013.
27. Carr MW, Roth SJ, Luther E, et al. Monocyte chemoattractant protein 1 acts as a T-lymphocyte chemoattractant. Proc Natl Acad Sci U S A 1994; 91:3652–3656.
28. Yang L, Froio RM, Sciuto TE, et al. ICAM-1 regulates neutrophil adhesion and transcellular migration of TNF-alpha-activated vascular endothelium under flow. Blood 2005;106:584–592.
29. Ma W, Zhang Y, Gao C, et al. Monocyte infiltration and proliferation reestablish myeloid cell homeostasis in the mouse retina following retinal pigment epithelial cell injury. Sci Rep 2017;7: 8433.
30. Zabel MK, Zhao L, Zhang Y, et al. Microglial phagocytosis and activation underlying photoreceptor degeneration is regulated by CX3CL1-CX3CR1 signaling in a mouse model of retinitis pigmentosa. Glia 2016;64:1479–1491.
31. Silverman SM, Wong WT. Microglia in the retina: roles in development, maturity, and disease. Annu Rev Vis Sci 2018;4:45–77.
32. Ansari AM, Ahmed AK, Matsangos AE, et al. Cellular GFP toxicity and immunogenicity: potential confounders in in vivo cell tracking experiments. Stem Cell Rev 2016;12:553–559.
33. Cerullo V, Seiler MP, Mane V, et al. Toll-like receptor 9 triggers an innate immune response to helper-dependent adenoviral vectors. Mol Ther 2007;15:378–385.
34. Mao SA, Glorioso JM, Nyberg SL. Liver regeneration. Transl Res 2014;163:352–362.
35. Arechederra M, Berasain C, Avila MA, et al. Chromatin dynamics during liver regeneration. Semin Cell Dev Biol 2019 [Epub ahead of print]; DOI: 10.1016/j.semcdb.2019.03.004.
36. Taylor AW. Ocular immune privilege. Eye (Lond) 2009;23:1885–1889.
37. Simpson E. A historical perspective on immunological privilege. Immunol Rev 2006;213:12–22.

38. Rutar M, Provis JM, Valter K. Brief exposure to damaging light causes focal recruitment of macrophages, and long-term destabilization of photoreceptors in the albino rat retina. Curr Eye Res 2010;35:631–643.

39. Tarallo V, Hirano Y, Gelfand BD, et al. DICER1 loss and Alu RNA induce age-related macular degeneration via the NLRP3 inflammasome and MyD88. Cell 2012;149:847–859.

40. Reichel FF, Dauletbekov DL, Klein R, et al. AAV8 can induce innate and adaptive immune response in the primate eye. Mol Ther 2017;25:2648–2660.

41. Marangoni D, Wu Z, Wiley HE, et al. Preclinical safety evaluation of a recombinant AAV8 vector for X-linked retinoschisis after intravitreal administration in rabbits. Hum Gene Ther Clin Dev 2014;25:202–211.

42. Kuzmin AI, Finegold MJ, Eisensmith RC. Macrophage depletion increases the safety, efficacy and persistence of adenovirus-mediated gene transfer in vivo. Gene Ther 1997;4:309–316.

43. Stein CS, Pemberton JL, van Rooijen N, et al. Effects of macrophage depletion and anti-CD40 ligand on transgene expression and redosing with recombinant adenovirus. Gene Ther 1998;5:431–439.

44. Nwanegbo E, Vardas E, Gao W, et al. Prevalence of neutralizing antibodies to adenoviral serotypes 5 and 35 in the adult populations of The Gambia, South Africa, and the United States. Clin Diagn Lab Immunol 2004;11:351–357.

45. Yang WX, Zou XH, Jiang SY, et al. Prevalence of serum neutralizing antibodies to adenovirus type 5 (Ad5) and 41 (Ad41) in children is associated with age and sanitary conditions. Vaccine 2016; 34:5579–5586.

46. Dalkara D, Byrne LC, Lee T, et al. Enhanced gene delivery to the neonatal retina through systemic administration of tyrosine-mutated AAV9. Gene Ther 2012;19:176–181.

47. Sun X, Pawlyk B, Xu X, et al. Gene therapy with a promoter targeting both rods and cones rescues retinal degeneration caused by AIPL1 mutations. Gene Ther 2010;17:117–131.

48. Wen XH, Shen L, Brush RS, et al. Overexpression of rhodopsin alters the structure and photoresponse of rod photoreceptors. Biophys J 2009;96:939–950.

49. Tan E, Wang Q, Quiambao AB, et al. The relationship between opsin overexpression and photoreceptor degeneration. Invest Ophthalmol Vis Sci 2001;42:589–600.

Received for publication July 8, 2019;
accepted after revision August 16, 2019.

Published online: August 28, 2019